Tumor Necrosis Factor Induces Hyperphosphorylation of Kinesin Light Chain and Inhibits Kinesin-mediated Transport of Mitochondria

Kurt De Vos,* Fedor Severin,‡§ Franky Van Herreweghe,* Katia Vancompernolle,* Vera Goossens,* Anthony Hyman,‡§ and Johan Grooten*

*Department of Molecular Biology, Flanders Interuniversity Institute for Biotechnology and Ghent University, B-9000 Ghent, Belgium; and ‡Cell Biology Program, European Molecular Biology Laboratory, D-69012 Heidelberg, Germany; and §Max-Planck Institute for Cell Biology and Genetics, D-01307 Dresden, Germany

Abstract. The molecular motor kinesin is an ATPase that mediates plus end-directed transport of organelles along microtubules. Although the biochemical properties of kinesin are extensively studied, conclusive data on regulation of kinesin-mediated transport are largely lacking. Previously, we showed that the proinflammatory cytokine tumor necrosis factor induces perinuclear clustering of mitochondria. Here, we show that tumor necrosis factor impairs kinesin motor activity and hyperphosphorylates kinesin light chain through activation of two putative kinesin light chain kinases. Inactivation of kinesin, hyperphosphorylation of kinesin light chain, and perinuclear clustering of mitochondria exhibit the same p38 mitogen-activated kinase dependence, indicating their functional relationship. These data provide evidence for direct regulation of kinesin-mediated organelle transport by extracellular stimuli via cytokine receptor signaling pathways.

Key words: microtubule • organelle • okadaic acid • mitogen-activated protein kinase • phosphorylation

Introduction

Conventional kinesin (KIF5), originally discovered in 1985 (Brady, 1985; Vale et al., 1985), is a tetramer of two kinesin heavy chains (KHCs)[1] and two kinesin light chains (KLCs). Three domains compose KHC: an NH_2-terminal motor domain containing the ATPase activity and the microtubule (MT)-binding sites (Yang et al., 1989); a central α-helical coiled-coil involved in dimerization (de Cuevas et al., 1992); and a COOH-terminal tail, which binds KLC (Diefenbach et al., 1998). The KHC-tail:KLC complex appears to be a crucial regulatory target, involved in interaction with cargo (Brady and Pfister, 1991; Stenoien and Brady, 1997; Khodjakov et al., 1998) and controlling the motor activity of the motor protein (Hackney et al., 1991; Verhey et al., 1998; Coy et al., 1999; Friedman and Vale, 1999; Rahman et al., 1999; Stock et al., 1999).

KHC and KLC are reversibly phosphorylated on serine residues in vivo, suggesting that phosphorylation is involved in kinesin regulation. Indeed, KHC of membrane-bound, presumably active kinesin is hyperphosphorylated in vivo (Lee and Hollenbeck, 1995) and kinesin phosphorylation by protein kinase A (PKA) in vitro increased kinesin ATPase activity and thus may stimulate transport (Matthies et al., 1993). However, phosphorylation by PKA also reduced binding of kinesin to synaptic vesicles suggesting to the contrary decreased vesicle transport (Sato-Yoshitake et al., 1992). In a different approach, using okadaic acid (OA) to drive hyperphosphorylation of kinesin in cytosolic extracts, McIlvain et al. (1994) showed hyperphosphorylation of three components of the kinesin complex, but not of KHC in correlation with increased kinesin activity in vitro. One of these associated proteins was recently identified as KLC, and hyperphosphorylation of this KLC isoform was sufficient to increase kinesin activity in vitro (Lindesmith et al., 1997). Similarly increased vesicle motility was observed in OA-treated CV-1 cells (Hamm-Alvarez et al., 1993). However, in these cells no hyperphosphorylation of kinesin-associated proteins could be demonstrated, suggesting an indirect effect of OA on kinesin activity (McIlvain et al., 1994). Also, in melanophores, melanocyte stimulating hormone-induced dispersion of melanosomes by kinesin-II was dependent on PKA

Address correspondence to Johan Grooten, Department of Molecular Biology, Flanders Interuniversity Institute for Biotechnology and Ghent University, K. L. Ledeganckstraat 35, B-9000 Ghent, Belgium. Tel.: 32 9 264 5310. Fax: 32 9 264 5348. E-mail: johan.grooten@dmb.rug.ac.be

Kurt De Vos' present address is Department of Biological Sciences, Columbia University, New York, NY 10027.

[1]*Abbreviations used in this paper:* 2-DE, two-dimensional gel electrophoresis; Ab, antibody; KHC, kinesin heavy chain; KLC, kinesin light chain; MAP, microtubule-associated protein; MAPK, mitogen-activated protein kinase; MT, microtubule; OA, okadaic acid; PKA, protein kinase A; TNF, tumor necrosis factor.

activity, but again was not accompanied by changes in kinesin-II phosphorylation (Reilein et al., 1998). Taken together, these studies put forward KLC as a target of phosphorylation-dependent regulation of kinesin, although the lack of conclusive data linking in vitro kinesin phosphorylation and kinesin activity in vivo makes it difficult to assess the relevance of this regulatory phosphorylation in intact cells.

Previously, we showed that stimulation of sensitive cells with the proinflammatory cytokine tumor necrosis factor (TNF) induces abnormal, perinuclear clustering of mitochondria from an evenly spread distribution throughout the cytoplasm, the mitochondria withdraw from the cell periphery and aggregate in an unipolar, perinuclear cluster. This clustering of mitochondria was MT-dependent and mimicked by SUK4 mAb-mediated immunoinhibition of conventional kinesin, suggesting that TNF-induced mitochondrial clustering is caused by impaired kinesin-mediated transport of mitochondria (De Vos et al., 1998). Here, we show that TNF receptor-I induces activation of kinase pathways, resulting in hyperphosphorylation of KLC and inhibition of kinesin activity. These results provide a molecular basis for the previously reported perinuclear clustering of mitochondria.

Materials and Methods

Materials

Unless otherwise stated, all chemicals used in this study were purchased from Sigma-Aldrich.

Cell Culture and Stimulation

L929 cells were cultured as described (De Vos et al., 1998) and were typically stimulated for 1 h with 1,000 IU/ml murine TNF (specific activity of 1.98 IU/mg of protein, purified in our laboratory). Where needed, SB203580 (10 μM; Alexis Biochemicals) was added to the cells 2 h before stimulation with TNF.

Analysis of Mitochondrial Distribution

The distribution of the mitochondria was analyzed with a Zeiss LSM 410 microscope as described (De Vos et al., 1998). Rhodamine 123 (Molecular Probes) was excited at 488 nm and detected with a 525–540 nm band pass filter. At regular times after stimulation, CLSM images from four randomly chosen microscopic fields, each containing ~60 cells, were recorded. Clustering of mitochondria was represented as the mean of the frequency of the clustered phenotype of four fields (number of viable cells with clustered mitochondrial phenotype/total number of viable cells). Digital processing and color adjustment of the images was done using Corel Photo-Paint software.

Preparation of Total Cell Lysate and Microtubule-associated Protein (MAP)-depleted Cytosol

Total Cell Lysate. Suspension cultures of L929 cells were harvested and washed three times with ice-cold TBS to remove culture medium. The cell pellet was resuspended in 0.9 vol of lysis buffer (35 mM K-Pipes, 5 mM $MgSO_4$, 5 mM EGTA, 0.5 mM EDTA, 1 mM DTT, pH 7.4; PMEE) supplemented with phosphatase inhibitors (NaF, β-glycerophosphate, and vandadate), protease inhibitors (Complete™ EDTA-free; Boehringer), and 1% CHAPS, and left on a rotor for 10 min at 4°C. The lysate was clarified by centrifugation at 20,800 *g* for 15 min at 4°C. The protein concentration was determined by the Bradford method.

Undepleted Cytosol (In Vitro Kinase Assay). Suspension cultures of L929 cells were harvested and washed three times with ice-cold TBS to remove culture medium. The cell pellet was resuspended in PMEE lysis buffer supplemented with 0.03% digitonin (Merck), protease inhibitors, and phosphatase inhibitors, and shaken for 3 min at room temperature. The cytosol was recovered by centrifugation (20,800 *g*, 15 min, 4°C) and the protein concentration was estimated with the Bradford method.

MAP-depleted Cytosol (Motility Assays). Adherent L929 cell cultures were harvested by trypsinization and washed three times with cold PBS. The remainder of the procedure was performed at 4°C. The cell pellet was resuspended in 0.9 vol PMEE lysis buffer supplemented with 0.25 mM sucrose and protease inhibitors (PMEES), followed by douncing (200 strokes). Unbroken cells and nuclei were removed by centrifugation at 3,000 *g* for 10 min followed by centrifugation at 200,000 *g* for 30 min to obtain the cytosolic fraction. Thereafter, the cytosol was MAP-depleted by MT affinity. Unlabeled MTs were polymerized from 50 μl purified tubulin (22 mg/ml) by 30 min incubation at 37°C in the presence of 1 mM GTP and 15 μl glycerol. After incubation, the MT-containing solution was adjusted to 200 μl with BRB80-Taxol buffer (80 mM K-Pipes, 1 mM GTP, 1 mM $MgCl_2$, pH 6.8, and 10 μM Taxol; Molecular Probes). Subsequently, the MTs were spun at 28 psi in an airfuge (Beckman Coulter) for 5 min and resuspended in 50 μl BRB80-Taxol. For MAP depletion, 50 μl of unlabeled Taxol-stabilized MTs was added to cytosol prepared from 8–10 × 10^7 L929 cells that was adjusted to 4 mM Mg-ATP to prevent binding of kinesin to the MTs. This cytosol-MT mix was incubated for 15 min at 37°C, followed by centrifugation (160,000 *g*, 20 min, 20°C) to remove the MTs and MT-associated MAPs. The MAP-depleted cytosol was kept on ice until use or snap-frozen in liquid nitrogen.

Isolation of Mitochondria

In Vitro Motility. Mitochondria of adherent L929 cell cultures were labeled with Mitotracker GreenFM (1 μM; Molecular Probes) for 30 min under culture conditions. The cells were harvested by trypsinization, transferred to 4°C, and washed twice with ice-cold PBS and once with ice-cold mitochondria lysis buffer (10 mM Hepes, 220 mM mannitol, 70 mM sucrose, 1 mM EDTA, and protease inhibitors, pH 7.4; MB). The cell pellet was resuspended in 0.9 vol of MB buffer and homogenized with a tissue grinder (pestle 19, Kontes, 100 strokes). Unbroken cells and nuclei were removed by centrifugation (3,000 *g*, 10 min 4°C), followed by pelleting of the mitochondria (13,000 *g*, 15 min, 4°C). The mitochondrial pellet was resuspended in MB buffer and kept on ice. Mitochondria were freshly isolated before each experiment and used within 3 h after isolation.

Western Blot Analysis. Adherent L929 cell cultures were harvested by trypsinization, transferred to 4°C, and washed twice with ice-cold PBS and once with ice-cold MB buffer. The cell pellet was resuspended in 0.9 vol of MB buffer and homogenized with a tissue grinder (pestle 19, Kontes, 100 strokes). Unbroken cells and nuclei were removed by centrifugation (3,000 *g*, 10 min, 4°C). A crude mitochondrial pellet was obtained by centrifugation for 15 min at 13,000 *g*. Resuspended mitochondria were transferred on top of a discontinuous sucrose gradient (1.6 M sucrose, 0.1% BSA, 1 mM EDTA, 10 mM KH_2PO_4, pH 7.4; 1.2 M sucrose, 0.1% BSA, 1 mM EDTA, 10 mM KH_2PO_4, pH 7.4), and centrifuged at 42,000 rmp in a SW50.1 rotor (Beckman Coulter) for 1.5 h at 4°C. Mitochondria were recovered at the 1.6 M/1.2 M interface, supplemented with 9 vol MB, and subsequently pelleted by centrifugation at 100,000 *g* in a 50Ti rotor (Beckman Coulter). The mitochondrial pellet was subsequently lysed in PMEE supplemented with 1% NP-40. Mitochondrial proteins were separated on 7.5% SDS-PAGE.

Immunoprecipitation

2 mg total cell lysate was precleared by addition of 50 μl 50% protein G–Sepharose (Amersham Pharmacia Biotech) in PMEE and rotation for 2 h at 4°C. 15 μg antibody (Ab) was added and the lysate–Ab mix was rotated for 2 h at 4°C before addition of 25 μl 50% protein G–Sepharose. After overnight rotation at 4°C, the immune complex was washed five times with PMEE lysis buffer without CHAPS. KHC and KLC were immunoprecipitated with SUK4 mAb (Ingold et al., 1988) and antipan-KLC (pAb against squid KLC, 35.1; BAbCO) Ab, respectively; mouse anti–hamster IgG (BD PharMingen) was used as control Ab.

In Vitro Kinase Assay

The kinesin immune complex was mixed with 10 μCi γ[P^{32}]ATP and, where needed, with cytosol (1–1.5 mg) in 250 μl. The reaction mix was incubated for 5 min at 37°C and the reaction was stopped by transfer to 4°C and extensive washing of the immune complex with lysis buffer. The pellet

was resuspended in SDS-loading buffer (New England Biolabs, Inc.) containing β-mercaptoethanol, boiled, and separated on 12.5% SDS-PAGE. The gel was dried on paper and the incorporation of P^{32} was analyzed with an FX PhosphorImager (BioRad).

In Vitro Motility

MT Gliding Assay. Glass coverslips (22 × 22 mm; No. 1 Gold Seal, Clay Adams) were sealed onto a glass slide (KTH 360; Propper Ltd.) using two lines of Apezion M grease (Roth) to make 10 μl perfusion chambers. 10 μl of 5 μg/μl MAP-depleted cytosol was perfused into the chamber and allowed to bind for 5 min at room temperature, followed by perfusion of 3 mg/ml casein. Rhodamine-labeled MTs (Hyman, 1991) were perfused into the chamber and allowed to bind 1 min before addition of motility buffer (4 mM ATP, 75 mM KCl in PMEE).

Mitochondrial Motility. Rhodamine-labeled, polarity-marked MTs were perfused into the chamber and allowed to bind for 5 min. Unbound MTs were washed away with 3 mg/ml casein, followed by blocking the chamber with casein for 1 min. Casein was washed away with PMEES and reaction mix containing 8 μl MAP-depleted cytosol (5 μg/μl), 3 μl isolated mitochondria, and 1 μl ATP/KCl stock solution (10 mM ATP, 750 mM KCl in PMEE) was perfused into the chamber.

Data Acquisition. The chambers were observed with a COHU CCD camera on a Zeiss Axiovert 10 at room temperature with a 63× Plan-APOCHROMAT lens using NIH-image software and a rhodamine (MTs) or fluorescein (mitochondria) filter set. In the gliding assay, MTs were observed for 4–5 min in 2- or 4-s time intervals. Mitochondria were observed for 2–4 min with 2- or 4-s time intervals. Movement of mitochondria was defined as linear motions over at least three time intervals. Velocity was determined using Retrac software written by Dr. N. Carter (http://mc11.mcri.ac.uk/Retrac/RT-home.html).

Two-dimensional Gel Electrophoresis (2-DE)

For 2-DE, 500 μg protein was isoelectrofocused on 18-cm immobilized PH-gradient strips (Amersham Pharmacia Biotech) ranging from pH 3 to pH 10, followed by SDS-PAGE on 6–16% gradient gels.

Western Blot Analysis

Proteins were transferred to PVDF membranes (Amersham Pharmacia Biotech) by wet electroblotting and processed for ECL (Amersham Pharmacia Biotech) detection. KHC was detected using SUK4 mAb (1 μg/ml), or anti-KIF5B Ab, followed by HRP-conjugated anti-mouse Ig or HRP-conjugated anti-rabbit Ig Ab (1/2,000; Amersham Pharmacia Biotech), respectively. KLC was detected with antipan-KLC Ab (1/4,000) and HRP-conjugated anti-rabbit Ig Ab. ECL detection was performed according to the manufacturer's protocol. In the case of 2-DE blots, KHC was analyzed on the same blots used earlier for ECL detection of KLC by NBT/BCIP detection with SUK4 mAb (1 μg/ml) and AP-conjugated anti-mouse Ig (Sigma-Aldrich).

Syringe Loading

L929 cells were syringe-loaded as described previously (De Vos et al., 1998).

Results

TNF Signaling Inhibits Conventional Kinesin

Previously, we reported that TNF receptor I signaling causes abnormal, perinuclear clustering of mitochondria, indicating inhibition of kinesin-mediated, plus end-directed transport of mitochondria (De Vos et al., 1998). To directly assess the influence of TNF signaling on molecular motor-mediated transport, we analyzed in vitro the activity of molecular motors present in MAP-depleted cytosolic extracts of L929 cells treated with TNF for 1 h. Motor activity was assayed by MT gliding mediated by immobilized cytosolic proteins and by motility of mitochondria on immobilized MTs in the presence of cytosol. We choose for MAP-depleted cytosol to prevent inhibition of motility

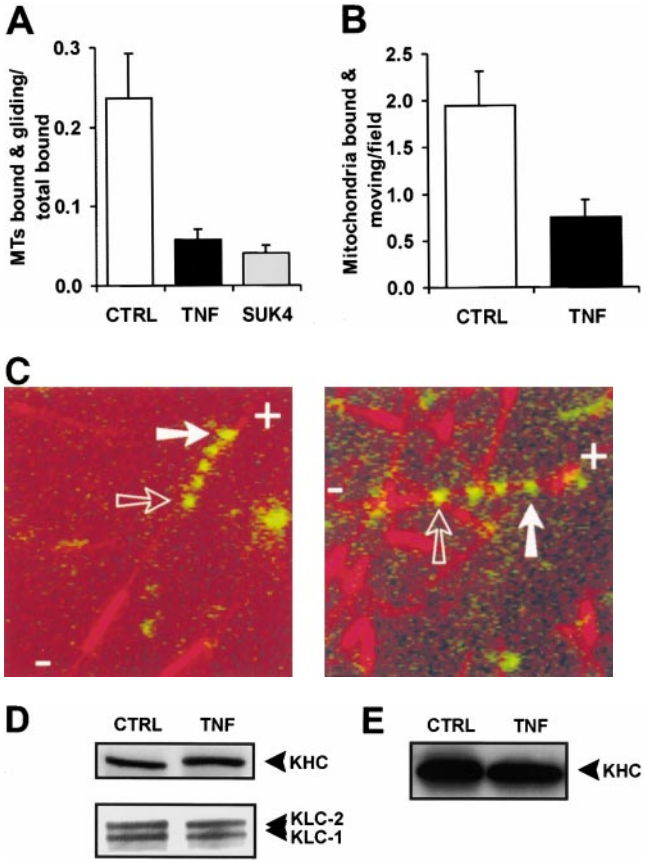

Figure 1. Inhibition of kinesin motor activity in TNF-treated L929 cells. A and B, MAP-depleted cytosol was prepared from untreated (CTRL) and TNF-treated (TNF) L929 cells and the level of kinesin motor activity in these preparations was tested in an MT-gliding assay (A) and a mitochondrial motility assay (B). In the MT-gliding assay, coverslips were coated with the respective cytosols, and rhodamine-labeled MTs were added together with ATP. The number of gliding MTs was determined relative to the total number of MTs present in a microscopic field. To identify the active molecular motor present in the untreated cytosol, SUK4 mAb was added (SUK4). Data shown are the mean and SEM calculated from at least ten different microscopic fields and are representative of a minimum of three independent experiments. The values of control and TNF samples were significantly different as determined using a one-tailed heteroscedastic *t* test ($P < 0.01$). In the mitochondrial motility assay, MTs were absorbed on coverslips and a reaction mix containing mitotracker-labeled mitochondria, ATP, and cytosol from untreated or TNF-treated L929 cells was added. The number of moving mitochondria per microscopic field was determined. The results shown represent the mean and SEM of 25 fields and are representative of three independent experiments ($P < 0.01$). C, The merged images of mitochondrial motility were generated by overlaying stacks of photos of mitochondria (green) collected at 4-s intervals with a photo of the immobilized MTs (red). The starting position of the mitochondria is indicated by the open arrow, the end position by the filled arrow. The plus end (+) and the minus end (–) of the MTs are indicated. D, The KHC and KLC content of the respective cytosols used in the gliding and mitochondrial motility assays was verified by Western blot with SUK4 mAb and antipan-KLC Ab, respectively. E, Mitochondria were purified from untreated (CTRL) and TNF-treated (TNF) L929 cells and the amount of copurifying KHC was determined by Western blot analysis using anti-KIF5B Ab.

by MT-bound MAPs (Heins et al., 1991; Lopez and Sheetz, 1993, 1995; Bulinski et al., 1997; Ebneth et al., 1998). Cytosol of untreated cells clearly contained active molecular motors capable of driving MT-gliding and mitochondrial motility in vitro (Fig. 1, A and B).

In the MT-gliding assay, MTs were typically observed for 4–5 min with 2- or 4-s time intervals. Use of polarity-marked MTs (Hyman, 1991) in the gliding assay allowed identification of the active motors in the untreated, MAP-depleted cytosol as plus end-directed (>95%), excluding the minus end-directed motors from the measurements. The average gliding velocity was 1.2 ± 0.03 μm/s. Furthermore, the observed plus end-directed activity could be nearly completely inhibited by addition of SUK4 mAb, a well-characterized mAb directed against the motor domain of conventional kinesin (Ingold et al., 1988), identifying the motor activity present in our lysates as conventional kinesin (Fig. 1 A).

In the mitochondria motility assay, mitochondria were observed for 2–4 min with 2- or 4-s time intervals. Movement was defined as linear motion along a MT over at least three time intervals. Typically, ~2% of the added mitochondria moved along the immobilized, polarity-marked MTs. Similar to the MT-gliding assay, 96% of the observed movements were plus end-directed. Mitochondria moved over an average distance of 4.92 ± 0.69 μm, with an average velocity of 0.59 ± 0.08 μm/s. Two typical examples are shown in Fig. 1 C.

When TNF-treated cytosol was applied, MT-gliding and mitochondrial motility were drastically reduced in comparison to the untreated control (Fig. 1, A and B). Western blot analysis showed that decreased MT-gliding and mitochondrial motility were not caused by reduced amounts of KHC or KLC in the cytosol preparations of TNF-treated cells (Fig. 1 D). Furthermore, no notable difference in the number of bound MTs between untreated and TNF-treated cytosol was observed in the gliding assay (data not shown). Diminished kinesin levels and/or impaired binding of kinesin to MTs can therefore be excluded as cause(s) of the lower number of gliding MTs in the TNF-treated condition. Also, the lower number of mitochondrial movements supported by TNF-treated cytosol could not be attributed to detachment of the motors from the organelles as the number of MT-bound mitochondria using TNF-treated cytosol did not significantly differ from the control (data not shown), and conventional kinesin copurified with mitochondria nearly equally in untreated and TNF-treated cells (Fig. 1 E). Therefore, we conclude that inactivation of kinesin motor activity, but not its MT- or cargo-binding activity, is responsible for inhibition of plus end-directed transport of mitochondria in TNF-treated L929 cells.

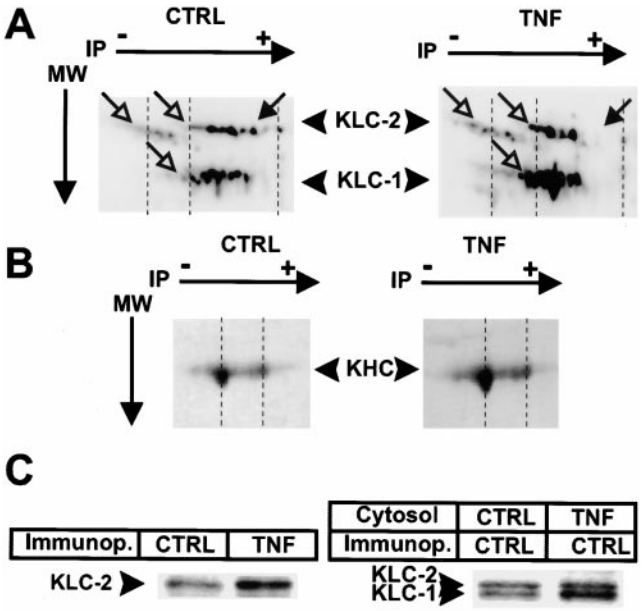

Figure 2. TNF induces hyperphosphorylation of KLC. A and B, Total lysates of untreated (CTRL) and TNF-treated (TNF) cells were separated by 2-DE (IP and MW) and transferred to PVDF membranes for Western blot analysis. KLC (A) and KHC (B) were revealed with antipan-KLC Ab and SUK4 mAb respectively. The filled arrow indicates isoelectric isoforms that disappear upon TNF-treatment. Open arrows indicate TNF-induced isoforms. C, KLC, coimmunoprecipitated with KHC (Immunop.) from untreated (CTRL) or TNF-treated (TNF) cells was incubated with $\gamma[P^{32}]$-ATP alone (left). Alternatively, KLC coimmunoprecipitated with KHC from untreated L929 cells was supplemented with cytosol of untreated or TNF-treated cells (right). After completion of the in vitro kinase assay, the immune complex was separated by SDS-PAGE. P^{32} incorporation was visualized by PhosphorImager.

TNF Signaling Induces Hyperphosphorylation of KLC

TNF is known to activate several kinases (including the mitogen-activated protein kinase [MAPK] family), leading to phosphorylation of various substrate molecules (Van Lint et al., 1992; Beyaert et al., 1996). As the MT-gliding and mitochondrial motility assay suggested a direct modulation of kinesin motor activity, we decided to investigate the phosphorylation state of conventional kinesin in TNF-stimulated cells. Lee and Hollenbeck (1995) showed that both KHC and KLC exist in several isoelectric forms in cultured cells and that these represent phosphoisoforms. Accordingly, we compared the relative abundance of these phosphoisoforms in untreated versus TNF-treated L929 cells by 2-DE and Western blot with anti-KHC mAb SUK4 or antipan-KLC Ab. In agreement with literature, we found that in L929 cells KHC and KLC exist in several isoforms, differing in both isoelectric point and molecular weight. Both KLC isoforms detected were named KLC1 and KLC2, according to Rahman et al. (1998). In TNF-treated cells, these isoforms showed a shift to more acidic isoelectric points (higher phosphorylation), whereas the isoelectric point distribution of KHC isoforms remained unchanged (Fig. 2, A and B). Thus, TNF signaling directly targets kinesin and, more particularly, KLC.

To verify if the increase in KLC phosphorylation in TNF-treated cells is the result of augmented kinase activity, we set up an in vitro kinase assay in which immunoprecipitated kinesin was used as substrate. To avoid interference of KLC-bound Ab with phosphorylation, KLC was coimmunoprecipitated with KHC using the KHC-specific SUK4 mAb rather than directly immunoprecipitated by

antipan-KLC Ab. Incubation of kinesin immunoprecipitates from untreated cells with $\gamma[P^{32}]$ATP in the absence of cytosol produced a background phosphorylation of KLC2 (Fig. 2 C, left), suggesting that KLC2 is phosphorylated by a constitutive kinesin-associated kinase. This is in agreement with Lindesmith et al. (1997) who also found that a KLC-isoform is directly phosphorylated by a kinesin-associated KLC kinase. KLC2 phosphorylation was clearly enhanced in coimmunoprecipitates from TNF-stimulated cells indicating increased activity of a putative kinesin-associated KLC2 kinase upon TNF-treatment (Fig. 2 C, left). Addition of cytosol of untreated cells produced additional phosphorylation of KLC1, indicating that KLC1 is phosphorylated by a specific cytosolic kinase distinct from the kinesin-associated KLC2 kinase. Cytosol of TNF-treated cells further enhanced phosphorylation of both KLCs, but especially of KLC1 (Fig. 2 C, right). Thus, both results from the in vitro kinase assay indicate that the hyperphosphorylation of KLC1 and KLC2 observed in TNF-treated cells is caused by enhanced kinase activity.

Remarkably, the in vitro assay did not reveal KHC phosphorylation (data not shown). This negative result, apparently in contradiction with the situation in L929 cells where several isoelectric isoforms of KHC were present, was not caused by the attached SUK4 mAb as in a reversed approach, using antipan-KLC Ab to coimmunoprecipitate KHC; also, no KHC phosphorylation was detected (data not shown). Apparently, KHC is already fully phosphorylated when immunoprecipitated and therefore no labeled phosphate is incorporated during the in vitro kinase assay.

We conclude that stimulation of L929 cells with TNF initiates a cytoplasmic signaling pathway leading to enhanced phosphorylation of KLC, but not KHC. KLC hyperphosphorylation apparently is caused by activation of two distinct KLC kinases, one cytosolic and the other kinesin-associated, which hyperphosphorylate KLC1 and KLC2, respectively.

Hyperphosphorylation of KLC Correlates with Inactivation of Kinesin and Perinuclear Clustering of Mitochondria

It has been shown that TNF activates PKA and the MAPK family (Zhang et al., 1988; Van Lint et al., 1992; Beyaert et al., 1996; Boone et al., 1998). While pharmacological studies showed that PKA does not phosphorylate kinesin in vivo (Hollenbeck, 1993), a recent report showed that the mixed lineage kinases, MLK2 and MLK3, associate with members of the KIF3 subfamily (Nagata et al., 1998), suggesting that MAPK may be involved in phosphorylation of kinesin. Overexpression of MLK2 activates, among others p38MAPK, which was shown to participate in TNF-signaling in L929 cells (Beyaert et al., 1996). Therefore we analyzed the role of p38MAPK in TNF-induced inhibition of conventional kinesin and KLC hyperphosphorylation.

2-DE analysis of KLC-phosphoisoforms from SB203580/TNF-cotreated L929 cells showed that application of SB-203580, a specific inhibitor of p38MAPK (Cuenda et al., 1995), inhibited the TNF-induced shift toward more acidic isoforms of KLC1 and KLC2 in vivo (Fig. 3 A). In the case of KLC2, SB203580 not only inhibited the TNF-mediated acidic shift, indicative for hyperphosphorylation, but also induced less acidic isoforms as compared with the control only treated with TNF, suggesting that p38MAPK is also involved in the constitutive activation of KLC2 kinase in TNF-treated cells. In vitro kinase assays confirmed these observations; KLC2 phosphorylation was no longer increased when conventional kinesin, immunoprecipitated from SB203580/TNF-cotreated cells, was incubated with $\gamma[P^{32}]$ATP (Fig. 3 B, left). Furthermore, the increment of KLC1 phosphorylation and, to a lesser extent, of KLC2 after incubation with cytosol from TNF-treated cells was no longer observed when cytosol from SB203580/TNF-cotreated cells was used instead (Fig. 3 B, right). Both results with cultured cells and in vitro results therefore indicate that p38MAPK is part of the TNF-induced signaling pathway leading to hyperphosphorylation of KLC1 and KLC2. In addition the lack of effect of SB203580 on the basal level of KLC phosphorylation in the in vitro kinase assay indicates that the putative TNF-induced KLC1 and KLC2 kinase activities are distinct from the kinase activities responsible for basal KLC phosphorylation. It is noteworthy that SB203580, per se, induced higher phosphorylation of KLC2 in L929 cells when compared with the untreated control shown in Fig. 2. However, this increase in phosphorylation was not observed in the in vitro kinase assay (Fig. 3 B). Therefore, it is likely this increase is not the result of enhanced kinase activity as in the case of TNF-induced KLC2 hyperphosphorylation, but might be caused by decreased phosphatase activity that is not detected in the in vitro kinase assay.

The inhibitory activity of the p38MAPK inhibitor, SB203580, on TNF-induced KLC phosphorylation provided us with a tool to investigate the relationship between TNF-induced KLC hyperphosphorylation and inhibition of kinesin activity. Kinesin activity in cytosol of SB203580/TNF-cotreated cells was directly measured with the MT-gliding and mitochondrial motility assays as described

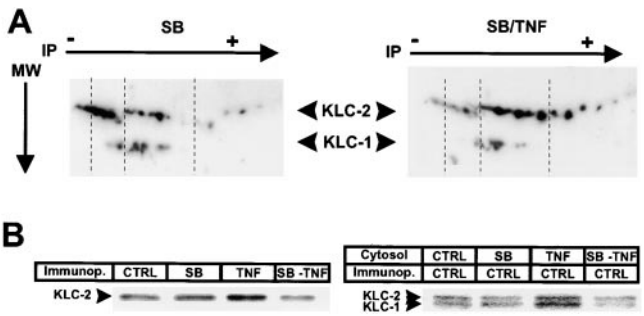

Figure 3. The p38MAPK inhibitor SB203580 inhibits TNF-induced KLC hyperphosphorylation. A, Total lysates of SB203580-treated (SB), and SB203580/TNF-cotreated (SB/TNF) L929 cells were separated by 2-DE, transferred to PVDF membranes, and were analyzed by Western blot with antipan-KLC Ab. B, KLC, coimmunoprecipitated with SUK4 mAb (Immunop.) from untreated (CTRL), SB203580-treated (SB), TNF-treated (TNF), or SB203580/TNF-cotreated (SB/TNF) L929 cells incubated with $\gamma[P^{32}]$-ATP alone (left) or supplemented with cytosol of the respective cell populations (right). Next, the immune complex was separated by SDS-PAGE and P^{32} incorporation was visualized by PhosphorImager.

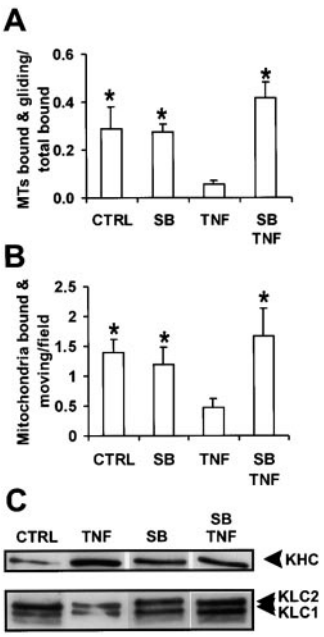

Figure 4. MT-gliding and motility of mitochondria are inhibited by SB203580. A and B, L929 cells were left untreated (CTRL), treated with SB203580 (SB) or TNF (TNF), or cotreated with SB203580 and TNF (SB/TNF). MAP-depleted cytosol was prepared and the activity of kinesin was tested in an MT-gliding assay (A) and a mitochondrial motility assay (B). *Values are not significantly different, as determined using a one-tailed heteroscedastic *t* test ($P > 0.06$). C, The KHC and KLC content of the respective cytosols used in the gliding and mitochondria motility assays was verified by Western blot with SUK4 mAb and antipan-KLC Ab, respectively.

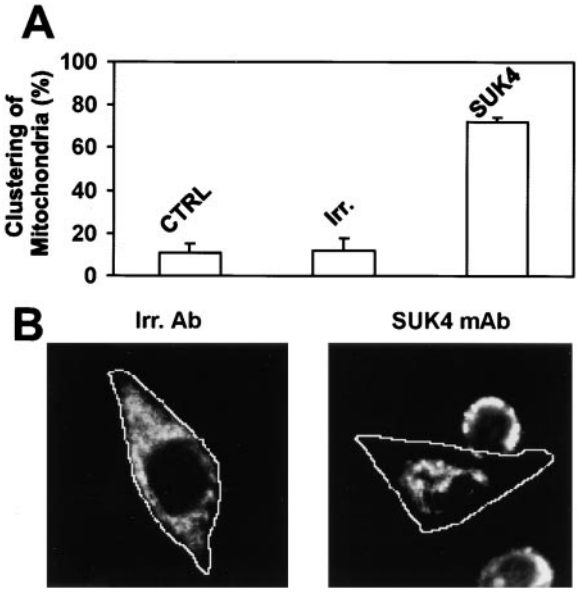

Figure 5. Conventional kinesin transports mitochondria in L929 cells. A, L929 cells were left unloaded (CTRL), or were syringe-loaded with irrelevant Ab (Irr.) or SUK4 mAb (SUK4). After overnight recovery of the cells, the distribution of R123-stained mitochondria was analyzed by CLSM in the cells that had taken up Ab. The values shown represent the mean and SEM of four randomly chosen microscopic fields each containing ~40 loaded cells. B, The SUK4 mAb-loaded cell typically shows a clustered distribution of mitochondria. In contrast, the irrelevant Ab-loaded cell retained the spread distribution of mitochondria. The line indicates the cell periphery.

above. In these assays, SB203580 neutralized the TNF effect. Thus, SB203580 restored MT-gliding and mitochondrial motility to control levels without affecting the amount of kinesin in the cytosol extracts nor MT-binding and organelle attachment (Fig. 4, and data not shown). Clearly, these TNF-induced parameters, hyperphosphorylation of KLC, and inhibition of kinesin activity, exhibited the same p38MAPK-dependence, indicating a functional relationship between these phenomena.

Three members of the kinesin superfamily have been implicated in transport of mitochondria, namely conventional kinesin (KIF5B; Tanaka et al., 1998), KLP67A (Pereira et al., 1997), and KIF1B (Nangaku et al., 1994). In L929 cells, inhibition of conventional kinesin by SUK4 mAb resulted in perinuclear clustering of mitochondria (Fig. 5, A and B; De Vos et al., 1998). This result indicates conventional kinesin mediates plus end-directed transport of mitochondria toward the cell periphery of L929 cells. In agreement, conventional kinesin is associated with mitochondria in L929 cells, as shown by Western blot analysis of purified mitochondria using anti-KIF5B Ab (Fig. 2 D). Since SB203580 reversed the TNF-induced inhibition of conventional kinesin in vitro, we verified whether inhibition of p38MAPK similarly could prevent TNF-induced clustering of mitochondria in vivo. Indeed, while SB203580, per se, did not influence the distribution of mitochondria in L929 cells, SB203580 completely prevented TNF-induced clustering of mitochondria (Fig. 6). Thus, both in vitro results and results obtained in L929 cells show that p38MAPK-dependent inhibition of conventional kinesin by TNF is at the basis of impaired plus end-directed transport of mitochondria and consequently clustering of mitochondria in L929 cells.

Discussion

In this study we investigated the involvement of the molecular motor kinesin in the previously described relocalization of mitochondria from an evenly spread distribution towards a perinuclear cluster, induced by TNF receptor-I signal transduction in sensitive cell lines such as L929 (De Vos et al., 1998). We provide data obtained in vitro and in cultured cells showing that TNF inhibits conventional kinesin in a p38MAPK-dependent way, likely by hyperphosphorylation of KLC. This inhibition arrested the motor activity of the protein, but not its MT-binding or mitochondria-binding activities. This result provides a molecular basis for the observed clustering of the mitochondria in L929 cells, namely repression of their plus end-directed transport through inhibition of conventional kinesin.

Current models propose that soluble kinesin is kept inactive in a folded conformation in which the KHC-tail: KLC complex is adjacent to the motor domain. Upon

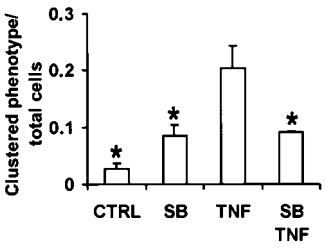

Figure 6. TNF-induced clustering of mitochondria is inhibited by SB203580. The frequency of cells exhibiting the clustered mitochondrial phenotype was measured by CLSM of R123-stained mitochondria 4 h after stimulation. The values shown represent the mean and SEM of four randomly chosen microscopic fields each containing ~60 cells. *Values are not significantly different as determined using a one-tailed heteroscedastic *t* test ($P > 0.07$).

binding to its cargo, kinesin unfolds and becomes activated. However, while several authors clearly showed that the KHC tail is involved in repression of KHC by folding of the KHC molecule (Coy et al., 1999; Friedman and Vale, 1999; Stock et al., 1999), the role of KLC in this folding-mediated repression of KHC is less clear. Although most reports show a contribution of KLC, KLC are not essential for folding-induced repression of KHC motility (Coy et al., 1999; Friedman and Vale, 1999; Stock et al., 1999). Moreover, other authors found that in KLC1-deficient cells, conventional kinesin accumulates at its normal site in the cell, although its activity is clearly inhibited (Rahman et al., 1999). This observation suggests that in absence of KLC, conventional kinesin can still bind to its cargo, but lacks a subsequent activating event involving KLC, which is consistent with our data showing that conventional kinesin copurifies with mitochondria from both untreated and TNF-treated cells, although its function is clearly inhibited in the latter case.

Our results provide evidence that a kinase cascade triggered by an extracellular stimulus, via the cytokine TNF, directly phosphorylates KLC and, in this way, may regulate kinesin-mediated transport of organelles. Considering the redundancy of kinase cascades triggered by various receptors in different cell types, it is likely that other extracellular stimuli can similarly modulate kinesin-mediated transport. However, depending on the cell type and its physiological situation, this modulation may be achieved through different mechanisms. Indeed, several reports described phosphorylation as regulator of kinesin-mediated transport in various cell systems. For example, increased anterograde transport during nerve growth factor-induced neurite outgrowth in PC12 cells is accompanied by augmented KHC phosphorylation (Lee and Hollenbeck, 1995). However, in this case it was speculated that the increase in KHC phosphorylation promoted enhancement of kinesin-mediated transport indirectly by shifting kinesin from its soluble state toward organelle association. We did not find any evidence supporting enhanced KHC phosphorylation, nor a shift toward organelle association and stimulation of organelle transport. Rather, our data document a correlation between inhibition of organelle transport and hyperphosphorylation of KLC without clear interference with organelle attachment and MT-binding. Thus, kinesin transport activity appears to be subject to complex phosphorylation-dependent regulation. KHC phosphorylation controls binding to cargo (allows unfolding of kinesin?), and p38MAPK-dependent KLC phosphorylation regulates the putative activation step upon binding to cargo. This model is in agreement with observations made in KLC1-deficient cells, which suggest that KLC are required for activation of kinesin when bound to its cargo (Rahman et al., 1999). Although this scheme is tempting, it might turn out to be an oversimplification. Indeed, hyperphosphorylation of a 79-kD KLC isoform enhances, instead of inhibits, the activity of kinesin (Lindesmith et al., 1997). However, in this study, phosphorylation of KLC was induced in vitro by the phosphatase inhibitor OA, whereas in our study, OA had no influence on TNF-induced KLC phosphorylation (data not shown). Furthermore, like McIlvain et al. (1994), we did not find increased KLC phosphorylation in OA-treated cells (data not shown). As several phosphorylation sites are present in KLC (Sato-Yoshitake et al., 1992), OA and TNF-signaling possibly induce KLC phosphorylation on other residues and elicit in that way opposite effects. A differential involvement of multiple KLC kinases may contribute to such an effect. Indeed, our observation that TNF-signaling induces phosphorylation of two KLC isoforms, KLC1 and KLC2, by activation of two isoform-specific kinases, whereas OA induces phosphorylation of only one KLC isoform, likely identical to KLC2, suggests that KLC1-specific kinase could be the differential factor in the TNF-pathway. Accordingly, the difference between our observations and those of others probably reflects the complexity and interplay of the regulatory pathways that control kinesin-mediated transport. Additionally, (phosphorylation of) nonmotor proteins such as MAPs were implicated in regulation of organelle transport (Heins et al., 1991; Lopez and Sheetz, 1993, 1995; Bulinski et al., 1997; Ebneth et al., 1998). However, immunoinhibition of conventional kinesin in L929 cells in the absence of TNF induced clustering of mitochondria similarly as observed in TNF-treated L929 cells. This strongly indicates that, as in the case of TNF treatment, repression of conventional kinesin is sufficient to generate mitochondrial clustering without requirement for other players. The vast knowledge on cytokine signaling provides us with well-characterized tools for future unraveling of the regulatory network governing organelle transport.

We would like to thank Dr. R. Vale (University of California at San Francisco) for providing anti-KIF5B Ab.

This study was supported partly by the Interuniversitaire Attractiepolen. K. De Vos received an EMBO short-term fellowship. V. Goossens is a postdoctoral fellow with the Fonds voor Wetenschappelijk Onderzoek Vlaanderen.

Submitted: 2 September 1999
Revised: 19 April 2000
Accepted: 1 May 2000

References

Beyaert, R., A. Cuenda, W. Vanden Berghe, S. Plaisance, J.C. Lee, G. Haegeman, P. Cohen, and W. Fiers. 1996. The p38/RK mitogen-activated protein kinase pathway regulates interleukin-6 synthesis response to tumor necrosis factor. *EMBO (Eur. Mol. Biol. Organ.) J.* 15:1914–1923.

Boone, E., V. Vandevoorde, G. De Wilde, and G. Haegeman. 1998. Activation of p42/p44 mitogen-activated protein kinases (MAPK) and p38 MAPK by tumor necrosis factor (TNF) is mediated through the death domain of the 55-kDa TNF receptor. *FEBS Lett.* 441:275–280.

Brady, S.T. 1985. A novel brain ATPase with properties expected for the fast axonal transport motor. *Nature.* 317:73–75.

Brady, S.T., and K.K. Pfister. 1991. Kinesin interactions with membrane bounded organelles in vivo and in vitro. *J. Cell Sci. Suppl.* 14:103–108.

Bulinski, J.C., T.E. McGraw, D. Gruber, H.L. Nguyen, and M.P. Sheetz. 1997. Overexpression of MAP4 inhibits organelle motility and trafficking in vivo. *J. Cell Sci.* 110:3055–3064.

Coy, D.L., W.O. Hancock, M. Wagenbach, and J. Howard. 1999. Kinesin's tail domain is an inhibitory regulator of the motor domain. *Nat. Cell Biol.* 1:288–292.

Cuenda, A., J. Rouse, Y.N. Doza, R. Meier, P. Cohen, T.F. Gallagher, P.R. Young, and J.C. Lee. 1995. SB 203580 is a specific inhibitor of a MAP kinase homologue which is stimulated by cellular stresses and interleukin-1. *FEBS Lett.* 364:229–233.

de Cuevas, M., T. Tao, and L.S.B. Goldstein. 1992. Evidence that the stalk of *Drosophila* kinesin heavy chain is an α-helical coiled coil. *J. Cell Biol.* 116: 957–965.

De Vos, K., V. Goossens, E. Boone, D. Vercammen, K. Vancompernolle, P. Vandenabeele, G. Haegeman, W. Fiers, and J. Grooten. 1998. The 55-kDa tumor necrosis factor receptor induces clustering of mitochondria through its membrane-proximal region. *J. Biol. Chem.* 273:9673–9680.

Diefenbach, R.J., J.P. Mackay, P.J. Armati, and A.L. Cunningham. 1998. The C-terminal region of the stalk domain of ubiquitous human kinesin heavy

chain contains the binding site for kinesin light chain. *Biochemistry*. 37: 16663–16670.

Ebneth, A., R. Godemann, K. Stamer, S. Illenberger, B. Trinczek, and E. Mandelkow. 1998. Overexpression of tau protein inhibits kinesin-dependent trafficking of vesicles, mitochondria, and endoplasmic reticulum: implications for Alzheimer's disease. *J. Cell Biol.* 143:777–794.

Friedman, D.S., and R.D. Vale. 1999. Single-molecule analysis of kinesin motility reveals regulation by the cargo-binding tail domain. *Nat. Cell Biol.* 1:293–297.

Hackney, D.D., J.D. Levitt, and D.D. Wagner. 1991. Characterization of alpha 2 beta 2 and alpha 2 forms of kinesin. *Biochem. Biophys. Res. Commun.* 174: 810–815.

Hamm-Alvarez, S.F., P.Y. Kim, and M.P. Sheetz. 1993. Regulation of vesicle transport in CV-1 cells and extracts. *J. Cell Sci.* 106:955–966.

Heins, S., Y.H. Song, H. Wille, E. Mandelkow, and E.M. Mandelkow. 1991. Effect of MAP2, MAP2c, and tau on kinesin-dependent microtubule motility. *J. Cell Sci. Suppl.* 14:121–124.

Hollenbeck, P.J. 1993. Phosphorylation of neuronal kinesin heavy and light chains in vivo. *J. Neurochem*. 60:2265–2275.

Hyman, A.A. 1991. Preparation of marked microtubules for the assay of the polarity of microtubule-based motors by fluorescence. *J. Cell Sci. Suppl.* 14: 125–127.

Ingold, A.L., S.A. Cohn, and J.M. Scholey. 1988. Inhibition of kinesin-driven microtubule motility by monoclonal antibodies to kinesin heavy chains. *J. Cell Biol.* 107:2657–2667.

Khodjakov, A., E.M. Lizunova, A.A. Minin, M.P. Koonce, and F.K. Gyoeva. 1998. A specific light chain of kinesin associates with mitochondria in cultured cells. *Mol. Biol. Cell.* 9:333–343.

Lee, K.D., and P.J. Hollenbeck. 1995. Phosphorylation of kinesin in vivo correlates with organelle association and neurite outgrowth. *J. Biol. Chem*. 270: 5600–5605.

Lindesmith, L., J.M. McIlvain, Jr., Y. Argon, and M.P. Sheetz. 1997. Phosphotransferases associated with the regulation of kinesin motor activity. *J. Biol. Chem*. 272:22929–22933.

Lopez, L.A., and M.P. Sheetz. 1993. Steric inhibition of cytoplasmic dynein and kinesin motility by MAP2. *Cell. Motil. Cytoskel.* 24:1–16.

Lopez, L.A., and M.P. Sheetz. 1995. A microtubule-associated protein (MAP2) kinase restores microtubule motility in embryonic brain. *J. Biol. Chem*. 270: 12511–12517.

Matthies, H.J., R.J. Miller, and H.C. Palfrey. 1993. Calmodulin binding to and cAMP-dependent phosphorylation of kinesin light chains modulate kinesin ATPase activity. *J. Biol. Chem*. 268:11176–11187.

McIlvain, J.M., Jr., J.K. Burkhardt, S. Hamm-Alvarez, Y. Argon, and M.P. Sheetz. 1994. Regulation of kinesin activity by phosphorylation of kinesin-associated proteins. *J. Biol. Chem*. 269:19176–19182.

Nagata, K., A. Puls, C. Futter, P. Aspenstrom, E. Schaefer, T. Nakata, N. Hirokawa, and A. Hall. 1998. The MAP kinase kinase kinase MLK2 co-localizes with activated JNK along microtubules and associates with kinesin superfamily motor KIF3. *EMBO (Eur. Mol. Biol. Organ.) J.* 17:149–158.

Nangaku, M., R. Sato-Yoshitake, Y. Okada, Y. Noda, R. Takemura, H. Yamazaki, and N. Hirokawa. 1994. KIF1B, a novel microtubule plus end-directed monomeric motor protein for transport of mitochondria. *Cell.* 79: 1209–1220.

Pereira, A.J., B. Dalby, R.J. Stewart, S.J. Doxsey, and L.S. Goldstein. 1997. Mitochondrial association of a plus end-directed microtubule motor expressed during mitosis in *Drosophila*. *J. Cell Biol.* 136:1081–1090.

Rahman, A., D.S. Friedman, and L.S. Goldstein. 1998. Two kinesin light chain genes in mice. Identification and characterization of the encoded proteins [published erratum appears in *J. Biol. Chem*. 1998. 273:24280]. *J. Biol. Chem*. 273:15395–15403.

Rahman, A., A. Kamal, E.A. Roberts, and L.S. Goldstein. 1999. Defective kinesin heavy chain behavior in mouse kinesin light chain mutants. *J. Cell Biol.* 146:1277–1288.

Reilein, A.R., I.S. Tint, N.I. Peunova, G.N. Enikolopov, and V.I. Gelfand. 1998. Regulation of organelle movement in melanophores by protein kinase A (PKA), protein kinase C (PKC), and protein phosphatase 2A (PP2A). *J. Cell Biol.* 142:803–813.

Sato-Yoshitake, R., H. Yorifuji, M. Inagaki, and N. Hirokawa. 1992. The phosphorylation of kinesin regulates its binding to synaptic vesicles. *J. Biol. Chem*. 267:23930–23936.

Stenoien, D.L., and S.T. Brady. 1997. Immunochemical analysis of kinesin light chain function. *Mol. Biol. Cell.* 8:675–689.

Stock, M.F., J. Guerrero, B. Cobb, C.T. Eggers, T.G. Huang, X. Li, and D.D. Hackney. 1999. Formation of the compact confomer of kinesin requires a COOH-terminal heavy chain domain and inhibits microtubule-stimulated ATPase activity. *J. Biol. Chem*. 274:14617–14623.

Tanaka, Y., Y. Kanai, Y. Okada, S. Nonaka, S. Takeda, A. Harada, and N. Hirokawa. 1998. Targeted disruption of mouse conventional kinesin heavy chain, kif5B, results in abnormal perinuclear clustering of mitochondria. *Cell.* 93:1147–1158.

Vale, R.D., T.S. Reese, and M.P. Sheetz. 1985. Identification of a novel force-generating protein, kinesin, involved in microtubule-based motility. *Cell.* 42: 39–50.

Van Lint, J., P. Agostinis, V. Vandevoorde, G. Haegeman, W. Fiers, W. Merlevede, and J.R. Vandenheede. 1992. Tumor necrosis factor stimulates multiple serine/threonine protein kinases in Swiss 3T3 and L929 cells. Implication of casein kinase-2 and extracellular signal-regulated kinases in the tumor necrosis factor signal transduction pathway. *J. Biol. Chem*. 267:25916–25921.

Verhey, K.J., D.L. Lizotte, T. Abramson, L. Barenboim, B.J. Schnapp, and T.A. Rapoport. 1998. Light chain-dependent regulation of kinesin's interaction with microtubules. *J. Cell Biol.* 143:1053–1066.

Yang, J.T., R.A. Laymon, and L.S.B. Goldstein. 1989. A three-domain structure of kinesin heavy chain revealed by DNA sequence and microtubule binding analyses. *Cell.* 56:879–889.

Zhang, Y.H., J.X. Lin, Y.K. Yip, and J. Vilcek. 1988. Enhancement of cAMP levels and of protein kinase activity by tumor necrosis factor and interleukin 1 in human fibroblasts: role in the induction of interleukin 6. *Proc. Natl. Acad. Sci. USA*. 85:6802–6805.